ChemPubSoc Europe
DOI: 10.1002/chem.201403988
CHEMISTRY
A European Journal
Full Paper

Carbenes |*Hot Paper*|

Quantitative Description of Structural Effects on the Stability of Gold(I) Carbenes

David H. Ringger, Ilia J. Kobylianskii, Daniel Serra, and Peter Chen*[a]

Abstract: The gas-phase bond-dissociation energies of a SO_2–imidazolylidene leaving group of three gold(I) benzyl imidazolium sulfone complexes are reported ($E_0 = 46.6 \pm 1.7$, 49.6 ± 1.7, and 48.9 ± 2.1 kcal mol^{-1}). Although these energies are similar to each other, they are reproducibly distinguishable. The energy-resolved collision-induced dissociation experiments of the three [L]–gold(I) (L = ligand) carbene precursor complexes were performed by using a modified tandem mass spectrometer. The measurements quantitatively describe the structural and electronic effects a *p*-methoxy substituent on the benzyl fragment, and *trans* [NHC] and [P] gold ligands, have towards gold carbene formation. Evidence for the formation of the electrophilic gold carbene in solution was obtained through the stoichiometric and catalytic cyclopropanation of olefins under thermal conditions. The observed cyclopropane yields are dependent on the rate of gold carbene formation, which in turn is influenced by the ligand and substituent. The donation of electron density to the carbene carbon by the *p*-methoxy benzyl substituent and [NHC] ligand stabilizes the gold carbene intermediate and lowers the dissociation barrier. Through the careful comparison of gas-phase and solution chemistry, the results suggest that even gas-phase leaving-group bond-dissociation energy differences of 2–3 kcal mol^{-1} enormously affect the rate of gold carbene formation in solution, especially when there are competing reactions. The thermal decay of the gold carbene precursor complex was observed to follow first-order kinetics, whereas cyclopropanation was found to follow pseudo-first-order kinetics. Density-functional-theory calculations at the M06-L and BP86-D3 levels of theory were used to confirm the observed gas-phase reactivity and model the measured bond-dissociation energies.

Introduction

Many reported homogeneous gold-promoted cyclopropanation reactions of olefins proceed by multistep pathways and presumably involve, as a key intermediate, a gold(I) carbene with carbocationic behavior.[1] Direct evidence for the existence of a gold(I) carbene intermediate has only very recently been accomplished by the isolation of a Fischer-type gold carbene.[1b,2] The synthesis of the normally highly reactive intermediates are accomplished primarily through cascade cycloisomerization,[3] diazo-compound decomposition,[4] and retrocyclopropanation reactions[5] by using π-acidic gold(I) salts and complexes. Many of these reactions work well, but the scope is often less broad then would be desired. A more thorough understanding of the elementary reaction steps and intermediates can help in the pursuit of an alternative, and possibly more versatile, route to the synthesis of positively charged gold(I) carbenes. The inter- or intramolecular cyclopropanation of alkenes to give cyclopropanes is reported in the literature and the trapping of carbenes with styrene is a well-known reaction model.[6]

Electrospraying a charged complex in a tandem mass spectrometer (ESI-MS/MS) and performing collision-induced dissociations (CID) with an inert gas allows not only the detection of charged reactive intermediates, but in the optimal case provides the means for bond-dissociation energy (BDE) measurements. Such thermochemical data helps in the interpretation of the steric and/or electronic effects of ligands, substituents, and leaving groups on product formation, which, in the best cases, is directly comparable to solution reactivity.[7] This method allows for more extensive mechanistic thinking and catalyst design, while decreasing the laborious trial-and-error approach. Furthermore, the measured gas-phase BDEs are directly comparable to density-functional-theory (DFT) modelling, and thus can validate the choice of functional and give confidence in its use for closely related complexes.[8]

Our group has been active in the application of ESI-MS/MS to obtain thermochemical data for a number of organometallic reactions, including olefin metathesis,[9] transmetalation,[10] palladium NHC-ligand dissociation,[11] cobalt–carbon bond energies,[12] coinage metal carbene formation,[13] and the gas-phase reactivity of an gold(I) carbene precursor complex, designated here as **C**, generated from a phosphonium ylid. The latter, however, proved unreactive in cyclopropanation reactions under thermal conditions in solution, which we attributed to a relatively strong carbon–phosphorus bond (51.7 kcal mol^{-1},

---

[a] D. H. Ringger, I. J. Kobylianskii, Dr. D. Serra, Prof. Dr. P. Chen
Laboratorium für Organische Chemie, ETH Zürich
Wolfgang-Pauli-Strasse 10, 8093 Zürich (Switzerland)
Fax: (+41) 44 632 1280
E-mail: peter.chen@org.chem.ethz.ch

Supporting information for this article is available on the WWW under http://dx.doi.org/10.1002/chem.201403988.

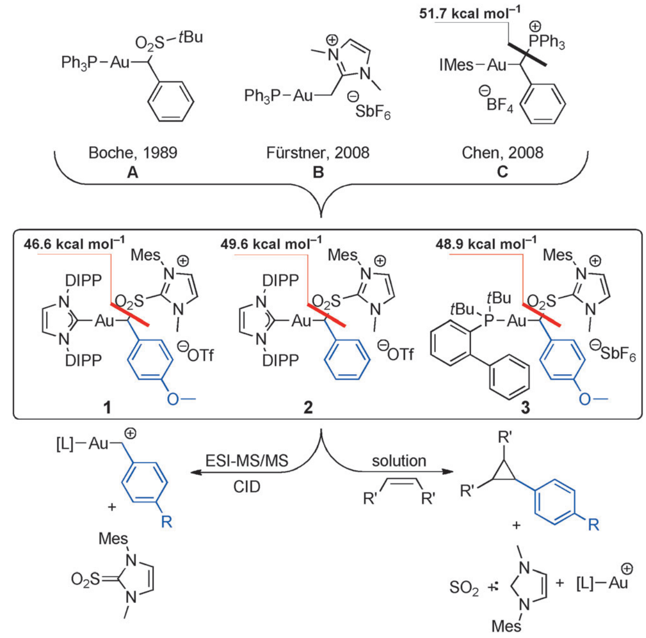

Scheme 1. Rational design of carbene precursors **1**–**3** based on previously reported gold(I) complexes. C–S bond-dissociation energies, gas-, and solution-phase reactivity of gold carbene precursor complexes **1**–**3**. IMes = 1,3-bis(2,4,6-trimethylphenyl)imidazole-2-ylidene, Mes = 2,4,6-trimethylphenyl, R = *p*-MeOC$_6$H$_4$ or H, DIPP = 2,6-diisopropylphenyl.

Scheme 1).[13a,b] We envisioned that appropriate modifications in the leaving group of the gold complex would give access to a gold carbene precursor complex that is reactive in catalytic cyclopropanation in solution.

Preliminary gas-phase investigation of charged gold alkyl complexes structurally analogous to **B**,[14] found that the carbon–imidazolium bond of these complexes was much stronger than the other bonds within the molecule. To weaken this bond, an SO$_2$ moiety was introduced to give a carbon–SO$_2$–imidazolium configuration comparable to that of the neutral and stable gold alkyl complex **A**.[15] The SO$_2$–imidazolylidene moiety acts as a leaving group, which further dissociates to give gaseous SO$_2$ and imidazolylidene.[16] The imidazolium function is desirable as it, not only provides the charge for gas-phase detection of the complex, but, in solution, its basic properties can be advantageous for a catalytic reaction during which catalytic amounts of base is required. Based on these considerations the gold complexes **1**, **2**, and **3** were synthesized and their carbene formation capabilities were investigated in the gas phase and in solution (Scheme 1).

Herein, we report the gas-phase energy-resolved collision-induced dissociation experiments of the SO$_2$–imidazolylidene leaving group, and the carbene cyclopropanation to an olefin in solution, of three [L]-gold(I) (L = ligand) carbene precursor complexes, **1**–**3**. The experimentally obtained gas-phase BDEs give an indication of whether the desired C–S bond breakage would occur competitively under thermal conditions, given the expected trends in solvation.[17] Additionally, these energies provide quantitative information regarding the steric and/or electronic effects a *p*-methoxy substituent on the benzylidene fragment and the *trans* [NHC] and [P] ligands have towards gold carbene formation. These results were compared to the obtained cyclopropane yields in the stoichiometric cyclopropanation reaction, along with a kinetic decomposition study of complex **1**. The measured BDEs and activation energies were also compared to DFT calculations at the M06-L and BP86-D3 level of theory.

The syntheses of the gold carbene complexes **1**–**3** were facile and accomplished in overall good yields (Scheme 2). 1-Mesityl-1*H*-imidazole was treated with *n*-butyl lithium and sulfur followed by the addition of an alkylating agent. The resulting intermediates were oxidized and the addition of methyl triflate yielded desired benzyl imidazolium sulfone salt **10**. Deprotonation of **10** and addition of [L]–gold(I)–acetonitrile gives the air-stable gold carbene precursor complexes **1**–**3**. The starting imidazole compound and alkylating agent can be varied easily, and thus allows for structurally diverse benzyl imidazolium sulfone salts. The corresponding anions of the complexes **1**–**3** are dependent on the gold starting material used. The synthesized gold complexes have a greater affinity to “soft” anions as described by the hard and soft acids and bases (HSAB) principle.[18] X-ray crystallography of complexes **1** and **3** provided not only an unambiguous structural assignment, but also located the associated anions. For more details, see the Supporting Information.

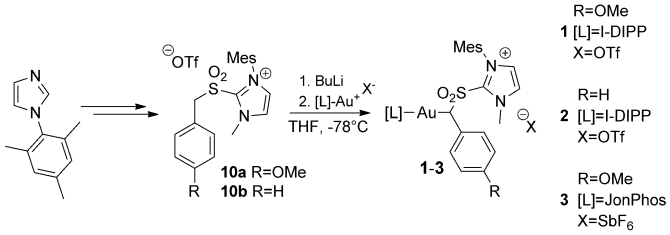

Scheme 2. Synthesis of gold carbene precursor complexes **1**–**3**. OTf = trifluoromethanesulfonate, X = BF$_4$ or SbF$_6$, I-DIPP = 1,3-bis(2,6-diisopropylphenyl)imidazol-2-ylidene, JonPhos = (2-biphenyl)-di-*tert*-butylphosphine.

It was suspected that complex **1** would be the best candidate for a catalytic cyclopropanation reaction due to the electron-rich *trans* [NHC] ligand and *p*-methoxy benzyl substituent. In our previous report, a mixture of complex **1**, the benzyl imidazolium sulfone salt **10a**, and *p*-methoxystyrene in CH$_2$Cl$_2$ at 120 °C gave the desired cyclopropane **11a** with up to 4.3 turnovers. In the proposed cycle (Scheme 3), the gold carbene cyclopropanates *p*-methoxystyrene, and the SO$_2$–imidazolylidene moiety further dissociates to give SO$_2$ and imidazolylidene **12**.[16] The latter acts as an in situ-formed base within the cycle and deprotonates another molecule of **10a**, which undergoes auration to restore gold complex **1**.[1a] This result is the starting point for the present study.

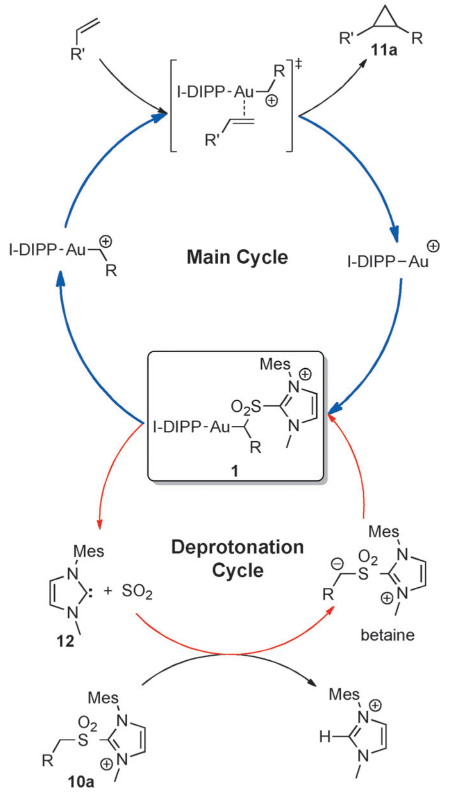

Scheme 3. Proposed catalytic cycle of gold carbene precursor complex **1**. The [gold(I) carbene···styrene]$^+$ transition state drawing is not meant to imply a preference for an inner-sphere over an outer-sphere carbene transfer mechanism, or vice versa. Triflate anions are omitted for clarity. R and R′ = *p*-MeOC$_6$H$_4$.

Results

Gas-phase reactivity

The evaluation of potential gold carbene precursor complexes was primarily accomplished by using an electrospray tandem mass spectrometer (ESI-MS/MS) as an assay tool. This spectrometer enables the direct detection and manipulation of any gold carbenes formed in the gas phase from potential precursors and selection of the most promising precursor complexes for a reaction in solution. The isolable and charged unimolecular gold carbene precursor complexes **1**–**3** are ideal for such a gas- and solution-phase comparison study because carbene formation presumably occurs by a single rate-determining step.

Collision-induced dissociation (CID) of the electrosprayed cationic [L]–gold(I) carbene precursor complexes **1**, **2**, and **3** (*m*/*z* = 970, 940, and 880, respectively) in a ESI-MS/MS, furnished two signals corresponding to 1) gold carbene **4**, **5**, and **6** (*m*/*z* = 706, 676, and 616, respectively) by loss of SO$_2$–imidazolylidene and 2) gold complex **7**, **8**, and **9** (*m*/*z* = 906, 876, and 816, respectively), the latter being generated through the extrusion of SO$_2$ from the starting gold complexes **1**–**3** (Figure 1). Notably, no gold–carbene–SO$_2$ adducts were observed, indicating that only the benzyl–sulfur bond is broken. The fate of the neutral SO$_2$–imidazolylidene leaving-group moiety could not be observed directly in the gas phase, but has been shown in solution to further dissociate to give SO$_2$ and imidazolylidene.[1a]

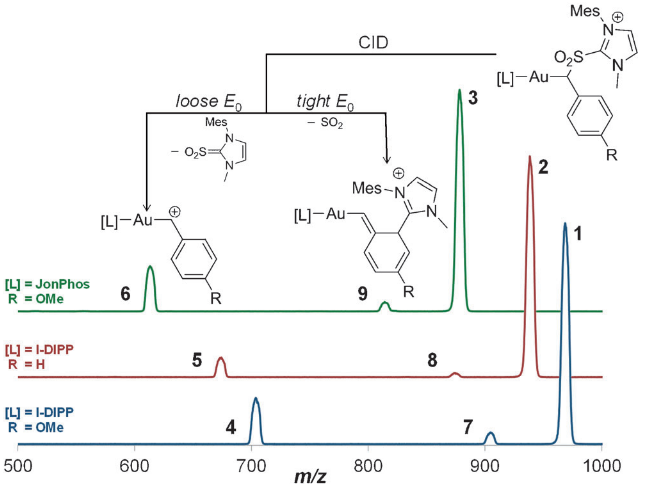

Figure 1. Relative intensity CID spectra of the gold carbene precursor complexes **1**–**3** at 6 eV velocity (center-of-mass reference frame) and 80 μTorr xenon. R = *p*-MeOC$_6$H$_4$ or H.

Taking into account that the gold carbene could, in principle, result from the rearranged gold complexes **7**–**9**, the spray settings were adjusted to generate what we presume to be **7**–**9** in the ion source. Upon mass selection and CID (Figure 2), a range of signals were observed corresponding to ligand loss and/or fragmentation. Only at very harsh collision conditions were minor amounts of gold carbene **4**–**6** observed, indicating that subsequent carbene formation from **7**–**9** has a much higher barrier.

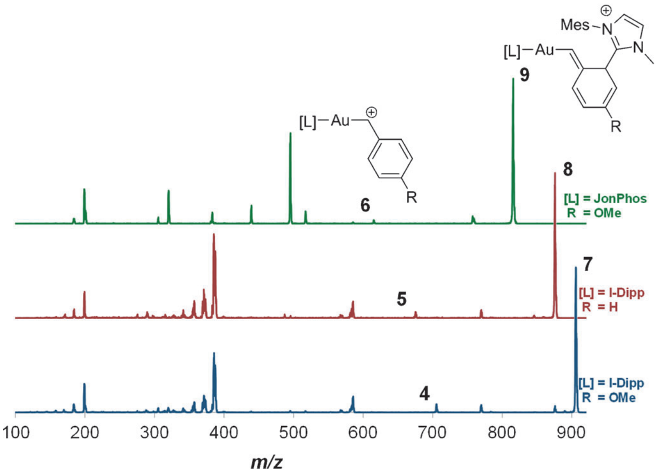

Figure 2. CID spectra of gold complexes **7**–**9** generated in the ion source. Spray voltage = 4500 V, capillary temperature = 175 °C, capillary offset = 200 V, tube lens offset = 200 V.

The detection of only two competing dissociation processes stemming from the same reactant ion renders complexes **1**–**3** suitable for two-channel energy-resolved threshold experiments. Thus, the benzyl–sulfur BDEs for gold carbene formation and the activation energies of the SO_2 extrusion can be determined.

CID threshold measurements

Acetonitrile solutions (10^{-6} mol L^{-1}) of the gold carbene precursor complexes **1**–**3** were electrosprayed into a customized Finnigan MAT TSQ-700 ESI-MS/MS spectrometer.[11] In a radiofrequency 24-pole ion guide, the reactant ions (**1**–**3**) were thermalized to the 70 °C manifold temperature with 10 mTorr argon gas, followed by mass selection at low resolution, to maintain a near-Gaussian kinetic energy distribution. Energy-resolved CID experiments were performed with low CID gas pressures (20–110 μTorr) to minimize multiple collisions. The reactant and product ion (**4**–**6**, **7**–**9**) intensities were recorded as a function of the collision offset of −80 to +10 eV in the lab frame energy, and the data curves fitted from 0 to up to 8.3 eV in the center of mass reference frame (see the Supporting Information for a full description of the experiment). The experiments were repeated on three separate days to confirm reproducibility. For each dataset, the signal intensities were converted to reactive collision cross sections,[11] and the single-collision contributions were extracted by extrapolation to zero pressure (Figure 1). The resulting curves were fitted with the L-CID program[19] (see the Supporting Information) previously developed within the group (Figure 3). To account for the correct treatment of the kinetic shift and other fitting parameters, the L-CID programrequires certain input assumptions, namely the transition-state models: "loose", if bond dissociation is rate limiting, or "tight" if intramolecular rearrangement prior to dissociation is rate limiting. Further input is the number of free rotors in the parent ions **1**–**3**.[20]

The loose transition-state model is appropriate for gold carbene formation **4**–**6** and the tight transition-state model is appropriate for the SO_2 extrusion rearrangement. The five free rotors consisting of the methyl groups and rotation about the gold–benzyl bond were determined by DFT analysis (only rotations <10 kcal mol^{-1} were considered) of the starting complexes **1**–**3** vibrational modes.

Varying the number of free rotors in the input file from 5 up to 18, representing the lower and upper boundaries based on the chemical structures (*p*-methoxy and *t*Bu or *i*Pr groups), increases the absolute E_0 energies by no more than 2–3 kcal mol^{-1}, but otherwise gives the same trends. The included error bounds contains the uncertainty in the fit from L-CID due to statistical scatter of the data points (see Table 1).

Although the absolute E_0 energies, with the statistical error bounds, for carbene formation **4**–**6** and rearrangement **7**–**9** overlap, the differences between them are distinct and reproducible.

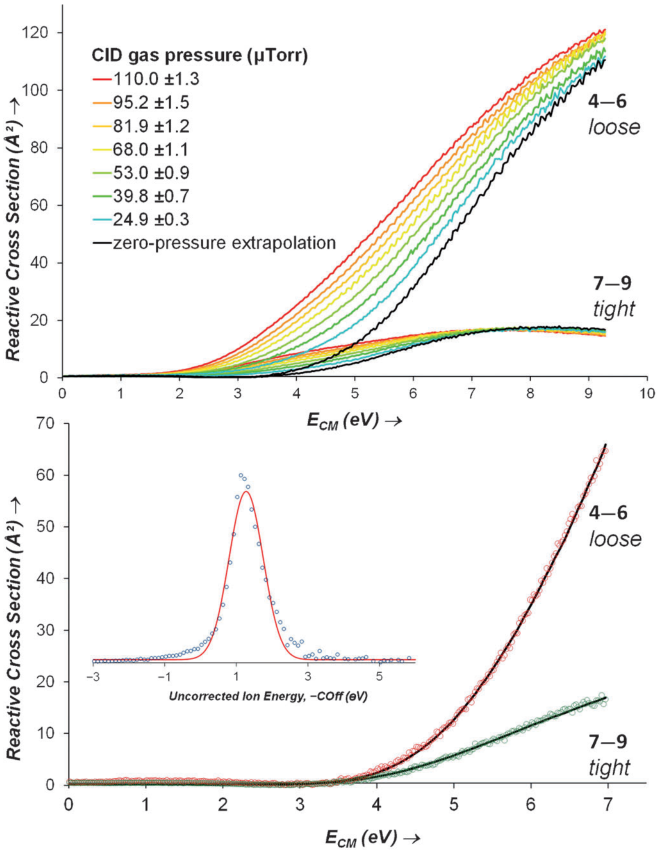

Figure 3. Top: Reactive cross sections (colored lines) and zero-pressure extrapolations (black lines) of the formation of ions **4**–**6** and **7**–**9**. Bottom: Truncated zero-pressure extrapolated curves (red and green dots) and averaged L-CID fitted curves (black lines). Inset: Kinetic-energy distribution (blue dots) and Gaussian fit (red line).

Table 1. LCID fitted results for the tight SO_2-extrusion rearrangement and loose gold carbene formation processes. Estimate of E_0 uncertainty of the fit is included.

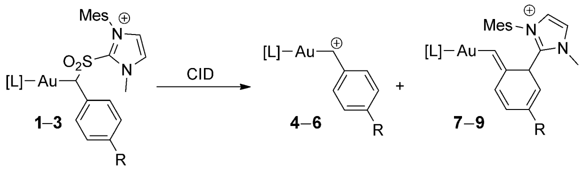

1–3

4–6

7–9

	Processes	**4**–**6** E_0 [kcal mol^{-1}] loose	**7**–**9** E_0 [kcal mol^{-1}] tight
[L]=I-DIPP R=OMe	**1**→**4**+**7**	46.6±1.7	25.6±1.3
[L]=I-DIPP R=H	**2**→**5**+**8**	49.6±1.7	29.3±2.1
[L]=JonPhos R=OMe	**3**→**6**+**9**	48.9±2.1	27.2±1.7

DFT calculations

Theoretically calculated electronic energies (corrected for zero-point energy), E_{el+ZPE}, were obtained to confirm the nature of the observed species, and for comparison with the experimentally determined activation energies E_0. Geometry optimizations were performed by using Gaussian 09[41] with M06-L/cc-pVDZ, with no imposed symmetry, tight geometry convergence criteria, tight SCF convergence criteria, and an ultrafine integration grid. Frequency analyses were carried out to confirm the nature of each stationary point. Single-point calculations in Gaussian 09 with the cc-pVTZ basis set were performed to improve the accuracy of the energies. Other functionals were evaluated by single-point energy calculations using the M06-L/cc-pVDZ geometries.

For our investigation of the loose bond-dissociation processes, we mainly used the M06-L functional because it has been designed to describe main-group and transition-metal thermochemistry, kinetics, and attractive dispersion effects between dissociating fragments.[21] Previously reported gas-phase and DFT studies involving gold carbene formation and gold aminonitrene dissociation have shown that the M06 functionals model the experimentally obtained data well.[13a,22] In particular, these functionals found C–S bond homolysis to be rate determining.

The localization of the tight SO_2 extrusion transition state required the evaluation of a few plausible reaction pathways. The transition state depicted in Figure 4 was found to be lowest in energy. However, M06-L appears to overestimate the SO_2 extrusion activation energy and we decided to benchmark other DFT functionals to assess their performance with respect to the investigated systems.

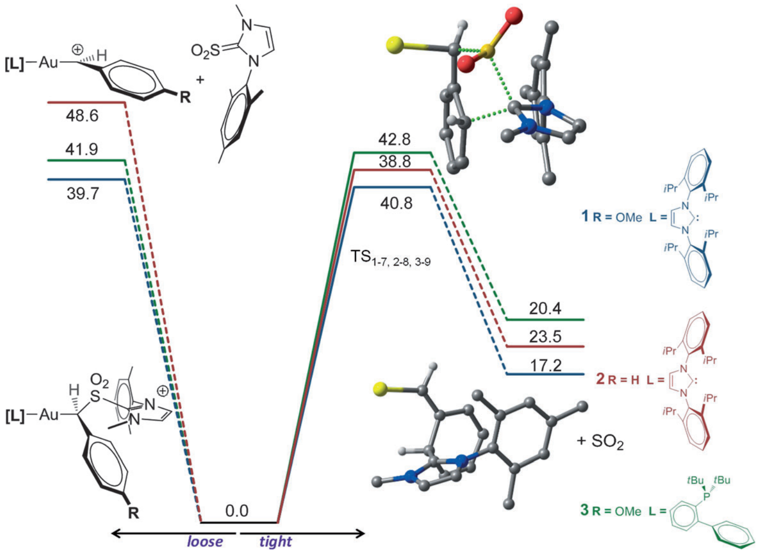

Figure 4. M06-L/cc-pVTZ//M06-L/cc-pVDZ potential-energy diagram of gold complexes **1**–**3**. Dashed lines denote dissociation reactions without reversible activation barriers. For the SO_2-rearrangement transition state and product, the ligands, hydrogen atoms, and *p*-methoxy substituent are omitted for clarity.

Some common DFT functionals were screened for the cc-pVTZ basis set, including the evaluation of Grimme's D3 dispersion correction,[23] as suggested for complexes of such sizes (Table 2).[24] For BP86, dispersion effects were found to affect both fragmentation channels significantly, but by different amounts. The starting complex **1** is stabilized by 25.6 kcal mol^{-1} with respect to carbene formation, and the SO_2 extrusion rearrangement transition state was found to be stabilized by 9.3 kcal mol^{-1} with respect to the starting complex (Figures 5 and 6).

Table 2. Measured and calculated relative energies [kcal mol^{-1}] for the formation of gold carbene (top) and rearranged (bottom) products.

Process	E_0 loose	M06-L[a]	M06[b]	BP86[c]	BP86-D3[d]
1→**4**	46.6 ± 1.7	39.7	40.4	19.8	45.4
2→**5**	49.6 ± 1.7	48.6	47.8	25.2	53.4
3→**6**	48.9 ± 2.1	41.9	42.5	19.8	47.2
Process	E_0 tight	M06-L[a]	M06[b]	BP86[c]	BP86-D3[d]
1→**7**	25.6 ± 1.3	38.8	40.8	40.8	31.5
2→**8**	29.3 ± 2.1	40.8	42.1	42.1	33.2
2→**9**	27.2 ± 1.7	42.8	44.8	44.8	35.2

[a] M06-L/cc-pVTZ//M06-L/cc-pVDZ single-point energies, including zero-point energy corrections. [b] M06/cc-pVTZ//M06-L/cc-pVDZ single-point energies, including zero-point energy corrections. [c] BP86/cc-pVTZ//M06-L/cc-pVDZ single-point energies, including D3-dispersion and zero-point energy corrections. [d] BP86-D3/cc-pVTZ//M06-L/cc-pVDZ single-point energies, including zero-point energy corrections.

Performance of the DFT functionals without treatment of dispersion effects can be described as poor and cannot be recommended for the investigation of similar systems. Inclusion of D3 treatment improves agreement between different methods and gives more accurate energy profiles with respect to experimental gas-phase data (Figure 1) for the loose and tight transition state. However, one should be careful with the inclusion of D3 corrections because it can mask other limitations of different functionals.

Solution-phase reactivity

The potential formation of gold carbenes **4**–**6** in solution was tested under conditions for the stoichiometric cyclopropanation of olefins.[1b–d] Heating complexes **1**–**3** to 120 °C in the presence of an excess of *p*-methoxystyrene in CH_2Cl_2 gives the expected **11** cyclopropane with variable yields (Table 3).

To probe the reactivity of the presumably formed gold carbene in solution, complex **1** was heated under argon in the presence of cyclohexene, a less reactive olefin (Scheme 4). The yield of cyclopropane **13** substantially decreased, but aside from the olefin, the only side products detected by gas chromatography (GC) were small amounts of benzaldehydes together with other unidentifiable products and purple colloidal gold. Heating complex

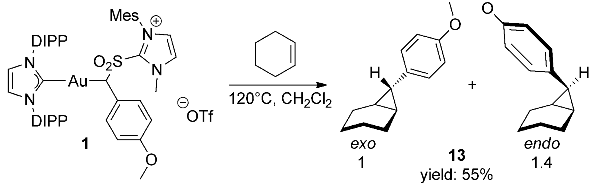

Scheme 4. Stoichiometric cyclopropanation of cyclohexene with gold carbene precursor complex **1**.

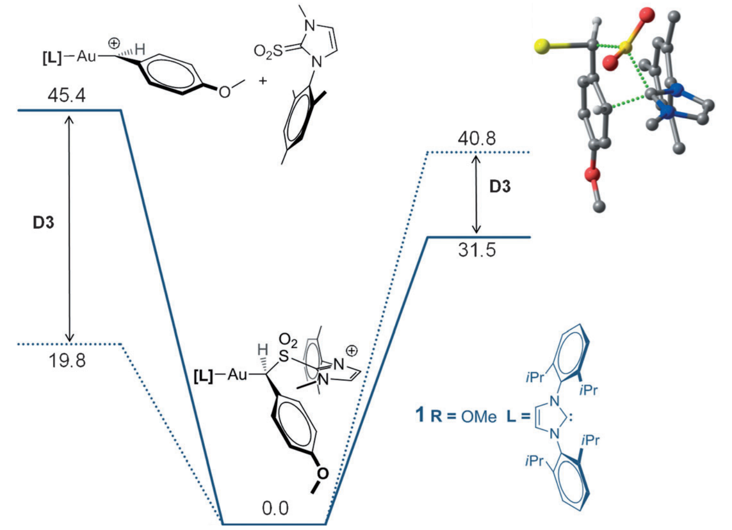

Figure 5. BP86/cc-pVTZ//M06-L/cc-pVDZ potential-energy surface diagram [kcal mol^{-1}] of complex **1**. The solid lines represent the D3-dispersion corrected energies. For the SO_2-rearrangement transition state, ligand and hydrogen atoms are omitted for clarity.

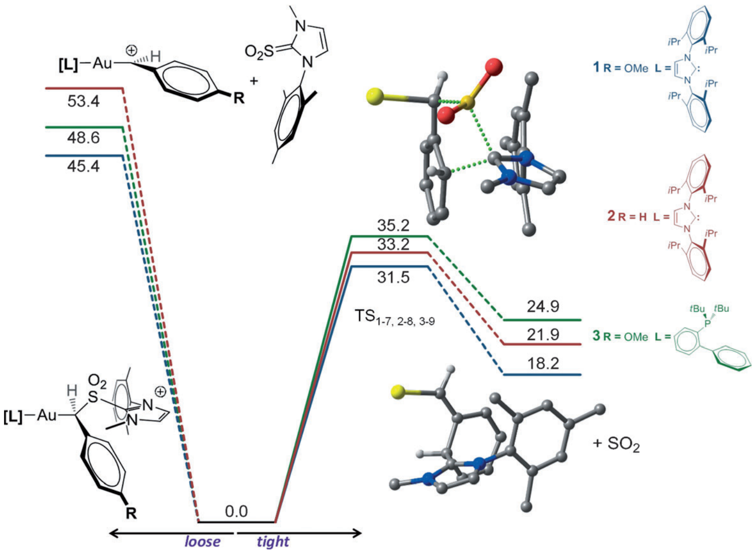

Figure 6. BP86-D3/cc-pVTZ//M06-L/cc-pVDZ potential-energy diagram [kcal mol^{-1}] of gold complexes **1**–**3**. Dashed lines denote dissociation reactions without reversible activation barriers. For the SO_2 rearrangement transition state and product, the ligand, hydrogen atoms, and *p*-methoxy substituent are omitted for clarity.

1 at 120 °C for 16 h, in the absence of an olefin, provided approximately 45 % *p*-methoxybenzaldehyde.[25]

To observe the expected unimolecular exponential decay of the gold carbene precursor complexes, a Schlenk flask was charged with **1**, a large excess of *p*-methoxystyrene, tetraoctylammonium tetrafluoroborate (internal standard), and cholorobenzene. The reaction mixture was then placed into a flask containing boiling *n*-butanol (118 °C) to ensure a much more stable temperature during the course of the experiment. The concentration of complex **1** was continuously monitored with a Thermo–Finnigan TSQ Quantum ESI-MS/MS spectrometer by using the pressurized infusion method setup as previously described by Vikse et al.[26] Additionally, a control experiment with the absence of *p*-methoxystyrene was conducted to probe the possible influence of the olefin.

Decomposition of complex **1** with and without the presence *p*-methoxystyrene follows expected first-order kinetics with a half-life of approximately 5.5–7 min (Figure 7). During the course of the reactions no other charged reactive intermediates were observed.

To monitor the evolution of cyclopropane **11a** in a stoichiometric cyclopropanation reaction, a setup as described above was used, but instead of electrospraying the reaction mixture into an ESI-MS/MS spectrometer, fractions were collected and analyzed by GC with flame-ionization detection (GC-FID).[27] The GC vials (in an automated fraction collector) were prefilled with hexane, which served to cool the reaction mixture to room temperature and immediately quench any subsequent chemistry. A Schlenk tube, fitted with a fused silica capillary, was charged with complex **1** in the presence of a large excess of *p*-methoxystyrene to ensure pseudo-first-order conditions, triphenylmethane (internal standard), and chlorobenzene. The Schlenk tube was then placed into a flask containing a boiling solvent to ensure a much more stable temperature during the course of the experiment. After collecting the fractions the GC samples were placed into a centrifuge before injecting them into the GC-FID (Figure 8). This experiment was repeated twice for three different temperatures using water, *n*-butanol, and chlorobenzene as boiling solvents.

It was found that the formation of cyclopropane **11a** follows pseudo-first-order kinetics with a rate constant of $\approx 1.9\times10^{-4}$–9.9×10^{-3} s^{-1}, consistent with the slope of the exponential decay of gold complex **1**. The Eyring equation was used to describe $\Delta G^{\ddagger}$,[28] $\Delta H^{\ddagger}$, and $\Delta S^{\ddagger}$,[29] which were found to be 27.8 ± 0.3, 36.0 ± 2.7 kcal mol^{-1}, and 21 ± 7 cal mol^{-1} K^{-1}, respectively.

The thermal decomposition of complexes **2** and **3** in CD_2Cl_2 at 120 °C were studied by using ^{1}H NMR spectroscopy. After heating complex **2** for 97 h, small amounts of starting complex, benzaldehyde, 3-mesityl-1-imidazolium, and substantial amounts of benzyl imidazolium sulfone salt **10b** were observed. In the case of complex **3**, the reaction was stopped after 3 h. After this time the starting complex has completely disappeared and small amounts of unidentifiable side products along with large quantities of *p*-methoxybenzaldehyde and 3-mesityl-1-imidazolium were observed. Further details are given in the Supporting Information.

Discussion

Within L-CID the type of transition state (loose or tight) is a required input and either assumption gives statistically acceptable fits for the two competing processes of carbene formation

Table 3. Stoichiometric cyclopropanation of gold carbene precursor complexes **1**–**3**.

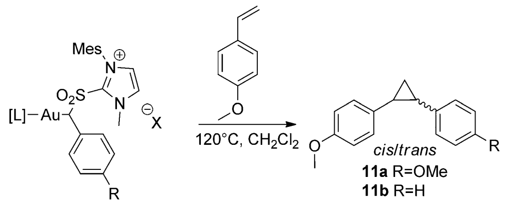

	Complex	Yield [%][a] *cis/trans*	Time [h]
1	[L] = I-DIPP R = OMe X = OTf	99 (14:1)	3
2	[L] = I-DIPP R = H X = OTf	5 (12: 1)	16
3	[L] = JonPhos R = OMe X = SbF_6	80 (14:1)	3

[a] GC yields relative to an internal standard.

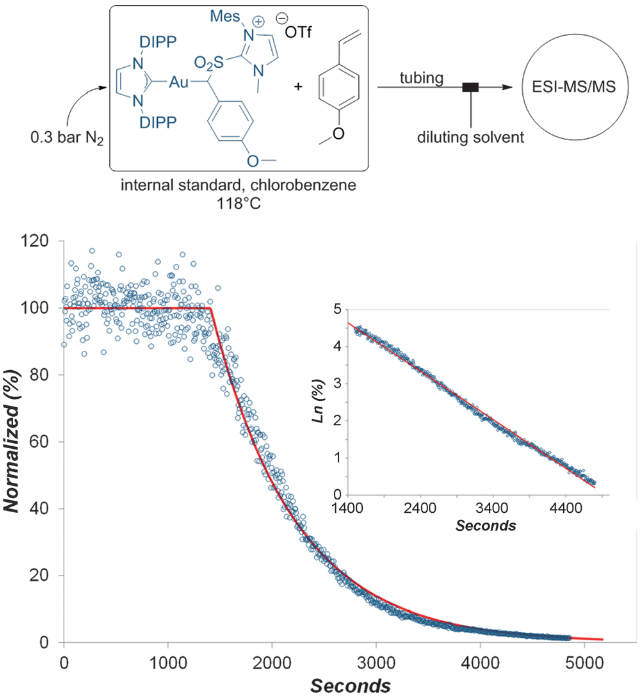

Figure 7. Normalized concentration of gold carbene precursor complex **1** (blue dots) versus time (seconds), exponential decay modelling (red line). At $t \approx 1400$ seconds the Schlenk tube containing the reaction mixture was placed into a flask containing boiling solvent, raising the temperature to start the reaction. Inset: Integrated first-order rate graph ln[A] versus time (seconds).

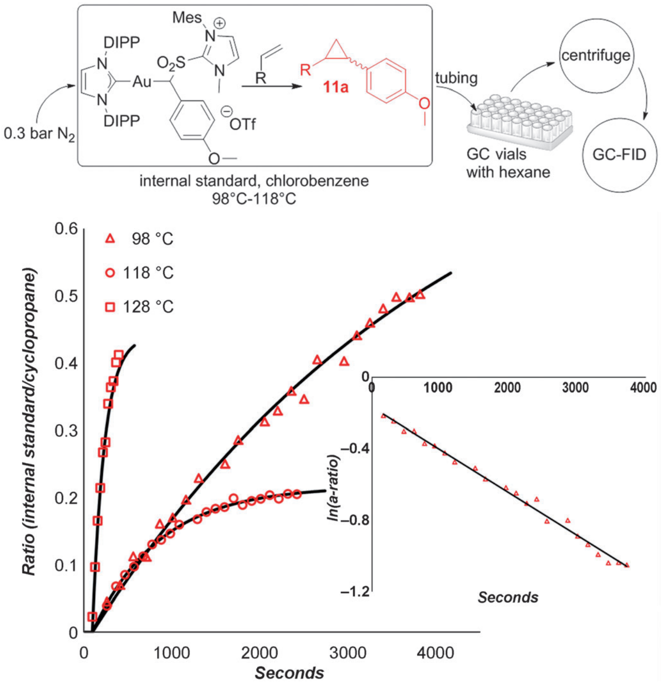

Figure 8. Ratio (cyclopropane/internal standard) (red symbols) versus time (seconds), logarithmic product formation modelling (black line). Inset: Integrated first-order rate graph ln[a-ratio] versus time (seconds). R = *p*-$MeOC_6H_4$.

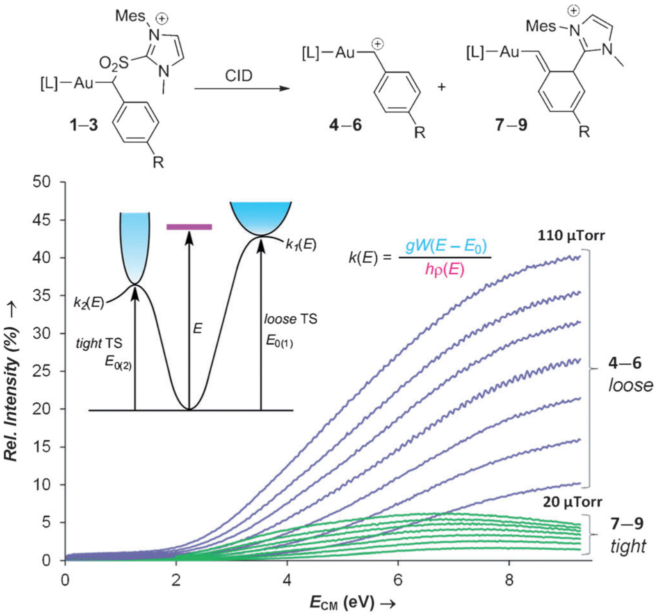

Figure 9. Recorded relative intensities as a function of the collision energy of the reactants **4**–**6** (purple) and **7**–**9** (green) at low CID gas pressures ranging from 110 to 20 µTorr. Inset: Statistical RRKM rate expression, and pictorial description of competitive loose and tight pathways as a function of the internal energy *E* of the reactant.

and SO_2 extrusion. However, based on chemical arguments and the shapes of the recorded relative intensity curves of the reactants (Figure 9), the appropriate transition-state models can be assigned unambiguously.

Specifically, the spectrometrically observed product ratios of the two competing processes can be explained by statistical Rice–Ramsperger–Kassel–Marcus (RRKM) theory (see Figure 9 inset). It defines the microcanonical rate constant of a process as a function of the internal energy *E*, in which *g* is the reaction degeneracy, $W(E–E_0)$ is the sum of states of the transition state with an energy less than or equal to $E\text{–}E_0$, h is Planck's constant, and $\rho(E)$ is the density of states for the energized starting ion at an energy E. The excess energy $E\text{–}E_0$ applied to the mass-selected ions is assumed to be statistically distributed over the accessible vibrational/rotational modes. For a loose dissociation transition state at the centrifugal barrier for the treatment of the dissociation in an ion-molecule reaction is modelled in L-CID. At the dissociation transition state, six vibrations in the energized reactant ion become three rotational and three translational modes, of which one translation is the reaction coordinate. The rate of a reaction with a loose transition state increases with excess energy much more quickly than that for a tight transition state. Consequently, the rate of a dissociation can exceed the rate of a rearrangement even if E_0 for the loose process is higher than E_0 of the tight process. Based on these arguments, one can often infer general features of the potential energy surface based on the observed behavior of the reaction cross-sections even before the extraction of activation barriers and/or consulting DFT calculations.[11,30]

Based on these arguments and on the inspection of the relative intensity of ions **4**–**6** and **7**–**9** as a function of collision energy (Figure 9), the appropriate transition-state model is loose for gold carbene formation **4**–**6** and tight for the SO_2-extrusion rearrangement **7**–**9** process (Table 1).

Having assessed the threshold CID curves qualitatively, and fitted by using L-CID, the obtained BDEs (Table 1) for complexes **1**–**3** allow the rationalization of the observed gas-phase reactivity for the different *para*-substituents and different *trans* [NHC] versus [P] ligand. The counterions can be ignored in the comparisons because the complexes exist as naked cations in the gas phase and there is no indication that the weakly coordinating anion is important to the reactivity in the moderately polar CH_2Cl_2 solution. Comparing complexes **1** and **2**, the formed carbene intermediate is stabilized by the donation of electron density from the *p*-methoxy benzyl substituent by up to 3 kcal mol^{-1}. The comparison of [NHC] and [P] ligand effects on carbene stabilization is less straightforward as the overall geometries are quite different. The approximately 2 kcal mol^{-1} BDE difference between complex **1** and **3** can, however, be regarded as an upper bound for the stabilization of the carbene owing to the electronic effects of the [NHC] ligand. It is generally accepted that [NHC] ligands are stronger σ donors, also exhibiting less $d \rightarrow \pi^*$ backbonding in comparison with [P] ligands. This is consistent with the experimentally observed stabilization of the electrophilic carbenes **4**–**6**.[24,31] The activation energies for the SO_2-extrusion rearrangement (Table 1, 25.6–29.3 kcal mol^{-1}) are surprisingly low when considering that aromaticity is disrupted, two C–S bonds are broken, and only one C–C bond is formed. Other pathways, for example, a three-membered cyclic transition state, have been considered, but the computed transition-state energies were considerably higher. An alternative, but higher energy transition state, is described in the Supporting Information. The SO_2-extrusion activation energies are, however, less interesting for our current study because this reaction is not kinetically competitive with the pathway leading to the cyclopropane in solution.[32,17] A literature search reveals that ionized organic sulfonyl compounds were also reported to extrude SO_2 in the gas phase. This reaction was suggested as a distinctive marker for the sulfonyl group. Thorough mechanistic studies are scarce, however, and it is difficult to make a direct comparison with our gold complexes **1**–**3**.[33] High resolution ESI-MS/MS of complexes **1**–**3** was conducted in order to validate the chemical formula of the product ions **4**–**6** and **7**–**9** (see the Supporting Information). The measured isotope patterns are in very good agreement with calculated patterns and confirm their identity. Structural evidence for the existence of gold carbenes in the gas phase has previously been reported by trapping experiments using complex **C**.[13a,b] The structures of the rearranged complexes **7**–**9** are DFT predictions.

With the reactive cross-section curves interpreted quantitatively, the measured thresholds energies were compared with the DFT-calculated energy barriers for carbene formation and SO_2 extrusion. The computed reaction pathways (Figure 4 and 6) predict benzyl–sulfur dissociation to proceed in a single step without a definable transition state up until the centrifugal barrier, whereas the SO_2-extrusion rearrangement follows a reaction with an initial tight transition state followed by SO_2 extrusion. The depicted transition states and products **7**–**9** are DFT predictions. It is also plausible that **7**–**9** further rearrange to restore aromaticity and form a product analogous to complex **B** (Scheme 1). However, experiments provide no evidence for or against these structures. The energies of the simple dissociation are in good agreement with the measured BDEs with M06-L, M06, and BP86-D3. Adding Grimme's D3-dispersion correction at the BP86 level greatly improved the calculations. In the case of complex **1** (Figure 5), the dispersion corrections increased the dissociation threshold by 25.6 kcal mol^{-1} and decreased the rearrangement barrier by 9.3 kcal mol^{-1}. However, in a solvation model the dispersion effects may be less pronounced.[34] The M06-family calculations are also in good agreement with the measured BDE of complex **2**, but they slightly overestimate the electronic contributions of the *p*-methoxy benzyl substituents in complexes **1** and **3**. Nevertheless, the calculated BDE difference of approximately 2 kcal mol^{-1} between **1** and **3** is in very good agreement with the measured BDE difference, reproducing the overall trend of benzyl–sulfur bond strengths. For the SO_2-extrusion activation energies, only the BP86-D3 calculated energies are in acceptable agreement with measurements, whereas M06 and M06-L consistently overestimate the height of the activation energies.

A summary of the key gas phase and DFT results is presented in Table 4, including the cyclopropanation yields observed in solution.

Having measured the carbene formation and SO_2-extrusion rearrangement energies in the gas phase and having confirmed the results by DFT, we now turn our attention to the accompanying solution-phase experiments. For the comparison of ease of carbene formation in terms of steric/electronic effects of the various structural modifications in both media, certain assumptions about the gold carbene precursor complexes **1**–**3** must be made. It is assumed that 1) carbene formation in the gas phase, and cyclopropanation in solution, of the three

Table 4. Summary of the measured thermochemical data, DFT calculations, and cyclopropanation yields.

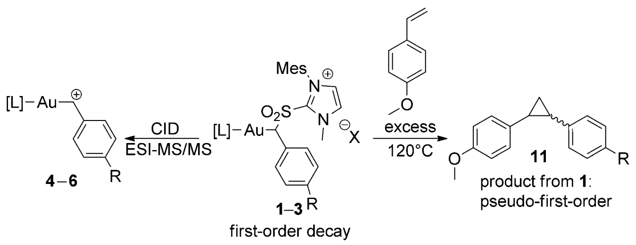

Complex	E_0 **4–6** [kcal mol^{-1}][a]	M06-L[b]	BP86-D3[c]	**11** Yield [%][d]
1 [L] = I-DIPP R = OMe X$^-$ = OTf	46.6 ± 1.7	39.7	45.4	99
2 [L] = I-DIPP R = H X$^-$ = OTf	49.6 ± 1.7	48.6	53.4	5
3 [L] = JonPhos R = OMe X$^-$ = SbF$_6$	48.9 ± 2.1	41.9	47.2	80

[a] BDEs threshold for gold carbene formation in kcal mol^{-1}. [b] M06-L/cc-pVTZ//M06-L/cc-pVDZ single-point energies, including zero-point energy corrections. [c] BP86-D3/cc-pVTZ//M06-L/cc-pVDZ single-point energies, including zero-point energy corrections. [d] GC yields relative to an internal standard.

complexes **1**–**3** follow analogous transition states, 2) carbene formation is the rate-determining step, 3) upon carbene formation, transfer to the electron rich *p*-methoxystyrene is quantitative and very rapid, 4) cyclopropanation follows pseudo-first-order kinetics with a steady-state olefin concentration and 5) solvation effects shift the absolute benzyl–sulfur bond energies of the three complexes in the same direction with similar magnitudes and the rate of carbene formation is reflected in cyclopropane yields. If these assumptions hold true, then we expect that the structural modifications are directly comparable to the gas-phase measured BDEs for carbene formation. The most reactive complex, **1**, exhibiting no other observable competitive decomposition pathways, was used to benchmark the other complexes, and to examine the assumptions made in points 2), 3), and 4).

To probe if the decay of the complexes **1**–**3** is rate limiting and follows first-order kinetics, the ESI-MS/MS pressurized infusion method described in Figure 7 was used to measure the thermal decay of complex **1**. The results revealed that carbene formation follows clean first-order kinetics with a half-life of 5.5–7 min.[35] No other charged intermediates were observed in the presence or absence of *p*-methoxystyrene. To confirm assumption number 3, complex **1** was used in a stoichiometric cyclopropanation reaction. This reaction gave the expected cyclopropane in quantitative yields (Table 4, 99%). Heating complex **1** in the absence of an olefin yields small amounts of unidentifiable products, but predominantly *p*-methoxybenzaldehyde. The aldehyde is most likely formed by oxidation of the gold carbene by SO$_2$.[25] The absence of 4,4′-dimethoxystilbene indicates that no homocoupling of two gold carbenes occurs, unlike what is commonly observed when using diazo compounds as carbene precursors.[36] These findings suggest that carbene formation is rate limiting for the overall cyclopropanation reaction, implying that the gold carbene is present only in small steady-state concentrations during the reaction, rendering homocoupling kinetically unfavorable. Consistent with this kinetic picture, cyclopropanation follows pseudo-first-order kinetics (Figure 8). Comparison of the results from the different kinetic-measurement techniques used in this study must be done with caution, but the rates are nevertheless as consistent with each other as one could expect. In any case, the first-order and pseudo-first-order kinetics of carbene formation and transfer are reproducible and unambiguous. The observed positive entropy of activation $\Delta S^{\neq}$ (Figure 8, 21 ± 7 cal mol^{-1} K^{-1}) in the GC-FID experiments is in accordance with the proposed rate-limiting carbene formation transition state. For comparison, a negative $\Delta S^{\neq} = -8.9$ cal mol^{-1} K^{-1} for carbene formation from ethyl diazoacetate and copper(I), measured by N$_2$ evolution,[37] suggests that the rate-determining step in that reaction could be coordination of the diazo compound to the metal, or some rearrangement in the complex.

Having established that the assumptions 1–4 are very likely to be correct, we turned our attention to assumption 5 and compared the ease of gold carbene formation in solution, measured by cyclopropanation yields, with the gas-phase BDEs for carbene formation. The observed cyclopropanation yields, resulting from precursor complexes **1**–**3**, exhibit dependency on the ligand *trans* to the carbene and on the *para* benzyl substituent (Table 4). The yields range from 5 to 99%, with complex **1** giving the highest yields, followed by **3** and then **2**. The gas-phase BDE differences seem small, but in principle a small increase of 2.3 kcal mol^{-1} in BDE decreases the rate of carbene formation by approximately 19 times[38] at the temperatures used in the cyclopropanation in solution. Hence, if no other competitive decomposition reactions are taking place, then carbene formation is quantitative if the reaction time is prolonged accordingly. However, replacing the [NHC] with a [P] ligand reduces the cyclopropane yields from 99 to 80%. In the absence of the *p*-methoxy substituent on the benzylidene, the yield drops further to 5%. The measured increase in BDE of complexes **2** and **3** decreases the rate of carbene formation to such an extent that eventually other decomposition pathways become competitive. The rate of carbene formation and transfer is most likely not influenced by the other decomposition pathways, but the final cyclopropane yields and overall decomposition rate of complexes **2** and **3** are. This effect is seen in complex **2**, which is slower in carbene formation, as evidenced by the fact that the starting complex was not completely decomposed after 97 h at 120 °C. Consequently, the rate of the dissociation of benzyl sulfone imidazolium moiety **10b** from [L]–gold(I) becomes competitive. Additionally, owing to the absence of an electron-donating *p*-methoxy substituent, the gold–benzyl bond is slightly weaker in complex **2** compared with **1**. This factor increases the rate of the dissociation of **10b** from complex **2** and makes the undesired decomposition pathway even more competitive. These observations could explain the absence of gold carbene formation for complex **C** in solution (Figure 1), for which the 51.7 kcal mol^{-1} BDE is a further 1.8 kcal mol^{-1} higher than in the worst case (complex **2**) in the current study. Although we cannot definitively exclude other factors, the trend is correct.

It has been suggested that carbene transfer to olefins can occur in a step-wise or concerted manner and may be dependent on the olefin. It was proposed that the electron-rich styrenes follow a step-wise mechanism, whereas the less-polarizable olefins follow a concerted pathway.[39] We used cyclohexene not only to probe the cyclopropanation scope, but also because different isomers might be observed if cyclopropanation followed a concerted versus a step-wise reaction mechanism (Scheme 4). If carbene transfer to cyclohexene followed a step-wise mechanism, there might be a chance to form isomers of cyclopropane **13** or polymerization products. However, heating complex **1** in the presence of cyclohexene only yielded 55 % of cyclopropane **13** and small quantities of *p*-methoxybenzaldehyde, which renders these results inconclusive for such an argument. Other trapping experiments and DFT calculations are needed for the investigation of the carbene-transfer transition state. The *cis* over *trans* and *endo* over *exo* selectivity is intriguing because the more sterically demanding product is observed. This phenomenon is, to date, unresolved and further experiments and DFT calculations are needed.

The reported results complement our previously communicated catalytic cyclopropanation reaction of complex **1** and highlight how the difference of a few kcal mol^{-1} in BDE can have an order-of-magnitude effect on the solution-phase kinetics for carbene formation and decomposition pathways.

Conclusion

The rationally developed gold carbene precursor complexes **1**–**3** were studied by collision-induced dissociation threshold measurements, along with DFT calculations and stoichiometric cyclopropanation reactions in solution. The measured benzyl–sulfur bond dissociation energies and SO_2-extrusion barriers of the three gold carbene precursor complexes were found to be dependent on the ligand *trans* to the carbene and on the *p*-methoxy benzyl substituent. The [NHC] ligand stabilizes the gold carbene intermediate by 2 kcal mol^{-1} and the *p*-methoxy benzyl substituent by 3 kcal mol^{-1}. These results support chemical intuition, which suggests that electron-donating groups on gold will stabilize the electrophilic carbene. It is a rare example of the quantitative assessment of reactive complexes without the usage of surrogate complexes. The DFT calculations for the BDEs at the M06-L and BP86-D3 level are in agreement with experimental results, whereas the SO_2-extrusion rearrangement barriers could only be modelled reasonably by using the BP86-D3 functional.

The ease of gold carbene formation in solution is reflected in the obtained cyclopropane yields, ranging from 5 to 99 %, and follow the same trend as the measured gas-phase BDEs, with complex **1** exhibiting the lowest BDE followed by **3** and **2**.

The expected unimolecular first-order decay of complex **1** was confirmed by using an ESI-MS/MS pressurized infusion method, and carbene transfer to the olefin was determined to follow pseudo-first-order kinetics.

The measured BDEs are useful for benchmarking future endeavors in the search for gold carbene precursors, which may be active in cyclopropanation. Further mechanistic investigation of the complexes **1**–**3** in cyclopropanation reactions will be reported in due course.

Experimental Section

General Procedures

Unless stated otherwise, all reactions were carried out under an atmosphere of argon by using standard Schlenk techniques with dried glassware and anhydrous solvents. Chromatographic purifications were carried out using neutral (pH 7.0) aluminum oxide. Thin-layer chromatography was carried out by using 0.2 mm layer of neutral aluminum oxide with UV_{254} indicator. NMR spectra were recorded on Mercury-vx 300, Amstrad DRX 400, and Avance III 600 spectrometers. Chemical shifts are given in ppm with respect to residual solvent resonances[40] and denoted by the following abbreviations: s (singlet), d (doublet), dd (double doublet), t (triplet), td (double triplet), sept (septet), m (multiplet). The high resolution ESI-MS/MS was performed by the MS service für Organische Chemie, ETH Zürich. The following chemicals were obtained from commercial sources and used without further purification, unless stated otherwise: 1,3-bis(2,6-di-*iso*-propylphenyl)imidazol-2-ylidene(acetonitrile)gold(I) tetrafluoroborate, (2-biphenyl)di-*tert*-butylphosphine(acetonitrile)gold(I) hexafluoroantimonate; *p*-methoxystyrene and cyclohexene were dried over CaH_2 and fractionally distilled under vacuum.

Synthesis of gold complexes 1–3

n-Butyl lithium (56 μmol) was slowly added to a solution of benzyl imidazolium sulfone salt **10** (56 μmol) in THF (0.5 mL) at −78 °C. The resulting yellow solution was stirred for 1 h at −78 °C before a solution of [L]–gold(I)–acetonitrile (56 μmol) in THF (0.5 mL) was added. The colorless solution was then stirred at −78 °C for 1 h and subsequently allowed to warm to room temperature and stirred for an additional 1 h. The mixture was then filtered through Celite and the filtrate concentrated in vacuo. The colorless oil was taken up in CH_2Cl_2 and purified by a short column chromatography with neutral alumina oxide (hexane, followed by a mixture of acetone/CH_2Cl_2 as eluent). The relevant fractions were combined and concentrated in vacuo to give the product (≈90 %) as white solid.

Typical procedure for the stoichiometric cyclopropanation reaction

A 5 mL Young Schlenk was charged, in a glovebox, with the gold carbene precursor **1**–**3** (3 μmol), olefin (150 μmol), and CH_2Cl_2 (1 mL). The resulting reaction mixture was stirred overnight in an oil bath at 120 °C. The mixture was then allowed to cool to room temperature and the internal standard (hexamethylbenzene) was added. The organic solvents were removed under a flow of nitrogen. The resulting oil was suspended in ≈2 mL of CH_2Cl_2/hexane 9:1 and filtered through a syringe filter. The resulting colorless solution was then injected into a GC-FID.

Procedure for the pressurized sample-infusion method

A 20 mL Schlenk was charged, in a glovebox, with complex **1** (1.2 mg, 1.0 μmol, 1.0 equiv), *p*-methoxystyrene (20 μL, 0.15 mmol, 150 equiv), and tetraoctylammonium tetrafluoroborate (2.5 mg, 4.5 μmol) in chlorobenzene (1 mL). The resulting reaction mixture was fitted with a fused silica tube (Ø = 100 μm) connected to a mixing T-piece, which was in turn connected to a syringe pump (benzene as diluting solvent) and ESI-MS/MS spectrometer that continuously recorded signal intensities of **1** and tetroctylammonium. The Schlenk was then placed into a preheated 120 °C oil bath and pressurized with 0.3 bar of N_2.

Procedure for the GC-FID kinetic measurement

A 10 mL Schlenk was charged in the glovebox with complex **1** (2 mg, 1.5 μmol, 1.0 equiv), *p*-methoxystyrene (30 μL, 0.22 mmol, 160 equiv), and triphenylmethane (1.0 mg) in chlorobenzene (2.5 mL). The resulting reaction mixture was fitted with a septum and a fused silica tube (Ø = 100 to 150 μm) connected to a fraction collector. 400–600 μL hexane was added to the GC vials and fractions were collected at a speed of 1–5 min depending on the temperature. The Schlenk tube was then placed into boiling solvent (water, *n*-butanol, and chlorobenzene) and pressurized with ≈0.3 bar of N_2.

Acknowledgements

The support from ETH Zürich and Swiss Nationalfonds is gratefully acknowledged. We thank Dr. Bernd Schweizer, Dr. Nils Trapp, and Michael Solar for the crystal structure determination; Louis Bertschi for the high resolution ESI-MS/MS; Dr. Erik P. A. Couzijn, Dr. Tim den Hartog, and Dr. Krista L. Vikse for useful discussions and Armin Limacher for synthetic support.

Keywords: bond-dissociation energies · carbenes · carbocations · cyclopropanation · density functional calculations · gold

[1] a) D. H. Ringger, P. Chen, *Angew. Chem.* **2013**, *125*, 4784 – 4787; *Angew. Chem. Int. Ed.* **2013**, *52*, 4686 – 4689; b) G. Seidel, R. Mynott, A. Fürstner, *Angew. Chem.* **2009**, *121*, 2548 – 2551; *Angew. Chem. Int. Ed.* **2009**, *48*, 2510 – 2513; c) D. Benitez, N. D. Shapiro, E. Tkatchouk, Y. Wang, W. A. Goddard, F. D. Toste, *Nature Chem.* **2009**, *1*, 482 – 486; d) A. M. Echavarren, *Nature Chem.* **2009**, *1*, 431 – 433; e) A. S. K. Hashmi, *Angew. Chem.* **2008**, *120*, 6856 – 6858; *Angew. Chem. Int. Ed.* **2008**, *47*, 6754 – 6756.

[2] a) G. Seidel, B. Gabor, R. Goddard, B. Heggen, W. Thiel, A. Fürstner, *Angew. Chem.* **2014**, *126*, 898 – 901; *Angew. Chem. Int. Ed.* **2014**, *53*, 879 – 882; b) R. E. M. Brooner, R. A. Widenhoefer, *Chem. Commun.* **2014**, *50*, 2420 – 2423.

[3] a) E. S. Jiménez-Núñez, A. M. Echavarren, *Chem. Rev.* **2008**, *108*, 3326 – 3350; b) A. Fürstner, L. Morency, *Angew. Chem.* **2008**, *120*, 5108 – 5111; *Angew. Chem. Int. Ed.* **2008**, *47*, 5030 – 5033; c) W. Rao, M. J. Koh, D. Li, H. Hirao, P. W. H. Chan, *J. Am. Chem. Soc.* **2013**, *135*, 7926 – 7932; d) P. Nösel, L. N. dos Santos Comprido, T. Lauterbach, M. Rudolph, F. Rominger, A. S. K. Hashmi, *J. Am. Chem. Soc.* **2013**, *135*, 15662 – 15666; e) E. Merino, C. Nevado, *CHIMIA* **2013**, *67*, 663 – 668; f) E. Rettenmeier, A. M. Schuster, M. Rudolph, F. Rominger, C. A. Gade, A. S. K. Hashmi, *Angew. Chem.* **2013**, *125*, 5993 – 5997; *Angew. Chem. Int. Ed.* **2013**, *52*, 5880 – 5884.

[4] M. R. Fructos, T. R. Belderrain, P. de Frémont, N. M. Scott, S. P. Nolan, M. M. Díaz-Requejo, P. J. Pérez, *Angew. Chem.* **2005**, *117*, 5418 – 5422; *Angew. Chem. Int. Ed.* **2005**, *44*, 5284 – 5288.

[5] a) C. S. R. Solorio-Alvarado, A. M. Echavarren, *J. Am. Chem. Soc.* **2010**, *132*, 11881 – 11883; b) C. s. R. Solorio-Alvarado, Y. Wang, A. M. Echavarren, *J. Am. Chem. Soc.* **2011**, *133*, 11952 – 11955; c) Y. Wang, P. R. McGonigal, B. Herlé, M. Besora, A. M. Echavarren, *J. Am. Chem. Soc.* **2014**, *136*, 801 – 809.

[6] a) T. d. Hartog, J. M. S. Toro, P. Chen, *Org. Lett.* **2014**, *16*, 1100 – 1103; b) D. F. Harvey, D. M. Sigano, *Chem. Rev.* **1996**, *96*, 271 – 288; c) M. P. Doyle, *Chem. Rev.* **1986**, *86*, 919 – 939; d) É. Lévesque, S. R. Goudreau, A. B. Charette, *Org. Lett.* **2014**, *16*, 1490 – 1493; e) H. Lebel, J.-F. Marcoux, C. Molinaro, A. B. Charette, *Chem. Rev.* **2003**, *103*, 977 – 1050; f) Y. Gai, M. Julia, J.-N. Verpeaux, *Bull. Soc. Chim. Fr.* **1996**, *133*, 817 – 829; g) S. Brandt, P. Helquist, *J. Am. Chem. Soc.* **1979**, *101*, 6473 – 6475.

[7] P. Chen, *Angew. Chem.* **2003**, *115*, 2938 – 2954; *Angew. Chem. Int. Ed.* **2003**, *42*, 2832 – 2847.

[8] a) L. Operti, R. Rabezzana, *Mass Spectrom. Rev.* **2006**, *25*, 483 – 513; b) P. B. Armentrout, *Int. J. Mass spectrom.* **2003**, *227*, 289 – 302; c) K. Eller, H. Schwarz, *Chem. Rev.* **1991**, *91*, 1121 – 1177; d) V. J. F. Lapoutre, B. Redlich, A. F. G. van der Meer, J. Oomens, J. M. Bakker, A. Sweeney, A. Mookherjee, P. B. Armentrout, *J. Phys. Chem. A* **2013**, *117*, 4115 – 4126.

[9] a) S. Torker, D. Merki, P. Chen, *J. Am. Chem. Soc.* **2008**, *130*, 4808 – 4814; b) Y.-Y. Lai, M. Bornand, P. Chen, *Organometallics* **2012**, *31*, 7558 – 7565.

[10] a) M.-E. Moret, D. Serra, A. Bach, P. Chen, *Angew. Chem.* **2010**, *122*, 2935 – 2939; *Angew. Chem. Int. Ed.* **2010**, *49*, 2873 – 2877; b) D. Serra, M.-E. Moret, P. Chen, *J. Am. Chem. Soc.* **2011**, *133*, 8914 – 8926.

[11] E. P. A. Couzijn, E. Zocher, A. Bach, P. Chen, *Chem. Eur. J.* **2010**, *16*, 5408 – 5415.

[12] I. J. Kobylianskii, F. J. Widner, B. Kräutler, P. Chen, *J. Am. Chem. Soc.* **2013**, *135*, 13648 – 13651.

[13] a) A. Fedorov, M.-E. Moret, P. Chen, *J. Am. Chem. Soc.* **2008**, *130*, 8880 – 8881; b) A. Fedorov, P. Chen, *Organometallics* **2009**, *28*, 1278 – 1281; c) L. Batiste, A. Fedorov, P. Chen, *Chem. Commun.* **2010**, *46*, 3899 – 3901; d) A. Fedorov, L. Batiste, A. Bach, D. M. Birney, P. Chen, *J. Am. Chem. Soc.* **2011**, *133*, 12162 – 12171.

[14] A. Fürstner, M. Alcarazo, R. Goddard, C. W. Lehmann, *Angew. Chem.* **2008**, *120*, 3254 – 3258; *Angew. Chem. Int. Ed.* **2008**, *47*, 3210 – 3214.

[15] a) H.-J. Kneuper, K. Harms, G. Boche, *J. Organomet. Chem.* **1989**, *364*, 275 – 279; b) B. Djordjevic, K. A. Porter, S. Nogai, A. Schier, H. Schmidbaur, *Organometallics* **2003**, *22*, 5336 – 5344.

[16] M. K. Denk, K. Hatano, A. J. Lough, *Eur. J. Inorg. Chem.* **2003**, 224 – 231.

[17] a) D. K. Bohme, G. I. Mackay, *J. Am. Chem. Soc.* **1981**, *103*, 978 – 979; b) E. D. Hughes, C. K. Ingold, *J. Chem. Soc.* **1935**, 244 – 255; c) M. R. J. Dack, *J. Chem. Educ.* **1974**, *51*, 231.

[18] R. G. Pearson, J. Songstad, *J. Am. Chem. Soc.* **1967**, *89*, 1827 – 1836.

[19] S. Narancic, A. Bach, P. Chen, *J. Phys. Chem. A* **2007**, *111*, 7006 – 7013.

[20] E. P. A. Couzijn, I. J. Kobylianskii, M.-E. Moret, P. Chen, *Organometallics* **2014**, *33*, 2889 – 2897.

[21] a) Y. Zhao, D. G. Truhlar, *J. Chem. Phys.* **2006**, *125*, 194101; b) Y. Zhao, D. G. Truhlar, *Acc. Chem. Res.* **2008**, *41*, 157 – 167; c) C. J. Cramer, D. G. Truhlar, *Phys. Chem. Chem. Phys.* **2009**, *11*, 10757 – 10816; d) D. G. Gusev, *Organometallics* **2013**, *32*, 4239 – 4243.

[22] a) A. Fedorov, E. P. A. Couzijn, N. S. Nagornova, O. V. Boyarkin, T. R. Rizzo, P. Chen, *J. Am. Chem. Soc.* **2010**, *132*, 13789 – 13798; b) A. Fedorov, L. Batiste, E. P. A. Couzijn, P. Chen, *ChemPhysChem* **2010**, *11*, 1002 – 1005.

[23] a) S. Grimme, J. Antony, S. Ehrlich, H. Krieg, *J. Chem. Phys.* **2010**, *132*, 154104; b) S. Grimme, S. Ehrlich, L. Goerigk, *J. Comput. Chem.* **2011**, *32*, 1456 – 1465.

[24] T. Risthaus, S. Grimme, *J. Chem. Theory Comput.* **2013**, *9*, 1580 – 1591.

[25] C. A. Witham, P. Mauleón, N. D. Shapiro, B. D. Sherry, F. D. Toste, *J. Am. Chem. Soc.* **2007**, *129*, 5838 – 5839.

[26] a) K. L. Vikse, M. P. Woods, J. S. McIndoe, *Organometallics* **2010**, *29*, 6615 – 6618; b) K. L. Vikse, Z. Ahmadi, C. C. Manning, D. A. Harrington, J. S. McIndoe, *Angew. Chem.* **2011**, *123*, 8454 – 8456; *Angew. Chem. Int. Ed.* **2011**, *50*, 8304 – 8306; c) K. L. Vikse, Z. Ahmadi, J. Luo, N. van der Wal, K. Daze, N. Taylor, J. S. McIndoe, *Int. J. Mass spectrom.* **2012**, *323–324*, 8 – 13.

[27] The GC-FID was standardized by using independently prepared authentic samples of **11a**. For more details, see the Supporting Information.

[28] ΔG was calculated from the measured rate constants by using the Eyring equation and the calculated uncertainty corresponds to one standard deviation.

[29] Plotting the six rate constants into an Eyring plot, the linear fit and multiple regression analysis yielded the thermodynamic data, including the one standard deviation error bands. For more details, see the Supporting Information.

[30] a) A. G. Brenton, R. P. Morgan, J. H. Beynon, *Annu. Rev. Phys. Chem.* **1979**, *30*, 51 – 78; b) T. Baercor, P. Mayerfn, *J. Am. Soc. Mass Spectrom.* **1997**, *8*, 103 – 115.

[31] a) M. Alcarazo, T. Stork, A. Anoop, W. Thiel, A. Fürstner, *Angew. Chem.* **2010**, *122*, 2596 – 2600; *Angew. Chem. Int. Ed.* **2010**, *49*, 2542 – 2546; b) S. Fantasia, J. L. Petersen, H. Jacobsen, L. Cavallo, S. P. Nolan, *Organometallics* **2007**, *26*, 5880 – 5889; c) D. Gatineau, J.-P. Goddard, V. Mouriès-Mansuy, L. Fensterbank, *Isr. J. Chem.* **2013**, *53*, 892 – 900.

[32] A difference in the activation barrier in solution versus gas phase results from the differential solvation of the reactant and the transition states. In agreement, we observe a decrease in ΔH for the carbene formation transition state of $\approx 11\ \text{kcal}\,\text{mol}^{-1}$ in our solution phase measurements.

[33] a) Z. Wang, C. E. C. A. Hop, M.-S. Kim, S.-E. W. Huskey, T. A. Baillie, Z. Guan, *Rapid Commun. Mass Spectrom.* **2003**, *17*, 81 – 86; b) N. Hu, P. Liu, K. Jiang, Y. Zhou, Y. Pan, *Rapid Commun. Mass Spectrom.* **2008**, *22*, 2715 – 2722.

[34] S. Schmidt, G. Abkai, T. Rosendahl, F. Rominger, P. Hofmann, *Organometallics* **2013**, *32*, 1044 – 1052.

[35] For the ESI-MS/MS pressurized infusion method the reaction mixtures were heated by using an oil bath. To ensure a stable temperature during the course of the GC-FID kinetic experiments, the reaction mixtures were heated in boiling solvents.

[36] a) X. Dai, T. H. Warren, *J. Am. Chem. Soc.* **2004**, *126*, 10085 – 10094; b) W. Baratta, A. Del Zotto, *Chem. Commun.* **1997**, 2163 – 2164.

[37] R. G. Salomon, J. K. Kochi, *J. Am. Chem. Soc.* **1973**, *95*, 3300 – 3310.

[38] The relative rates of carbene formation were estimated by using the Arrhenius equation and substituting E_a with the measured BDEs.

[39] a) M. J. Johansson, D. J. Gorin, S. T. Staben, F. D. Toste, *J. Am. Chem. Soc.* **2005**, *127*, 18002 – 18003; b) C. Obradors, A. M. Echavarren, *Chem. Commun.* **2014**, *50*, 16 – 28.

[40] G. R. Fulmer, A. J. M. Miller, N. H. Sherden, H. E. Gottlieb, A. Nudelman, B. M. Stoltz, J. E. Bercaw, K. I. Goldberg, *Organometallics* **2010**, *29*, 2176 – 2179.

[41] Gaussian 09, Revision D.01, M. J. Frisch, G. W. Trucks, H. B. Schlegel, G. E. Scuseria, M. A. Robb, J. R. Cheeseman, G. Scalmani, V. Barone, B. Mennucci, G. A. Petersson, H. Nakatsuji, M. Caricato, X. Li, H. P. Hratchian, A. F. Izmaylov, J. Bloino, G. Zheng, J. L. Sonnenberg, M. Hada, M. Ehara, K. Toyota, R. Fukuda, J. Hasegawa, M. Ishida, T. Nakajima, Y. Honda, O. Kitao, H. Nakai, T. Vreven, J. A. Montgomery, Jr., J. E. Peralta, F. Ogliaro, M. Bearpark, J. J. Heyd, E. Brothers, K. N. Kudin, V. N. Staroverov, R. Kobayashi, J. Normand, K. Raghavachari, A. Rendell, J. C. Burant, S. S. Iyengar, J. Tomasi, M. Cossi, N. Rega, J. M. Millam, M. Klene, J. E. Knox, J. B. Cross, V. Bakken, C. Adamo, J. Jaramillo, R. Gomperts, R. E. Stratmann, O. Yazyev, A. J. Austin, R. Cammi, C. Pomelli, J. W. Ochterski, R. L. Martin, K. Morokuma, V. G. Zakrzewski, G. A. Voth, P. Salvador, J. J. Dannenberg, S. Dapprich, A. D. Daniels, Ö. Farkas, J. B. Foresman, J. V. Ortiz, J. Cioslowski, and D. J. Fox, Gaussian, Inc., Wallingford CT, 2009.

Received: June 16, 2014